

NASA Technical Memorandum 85985

NASA-TM-85985 19840022157

---

# **$^3\text{He}$ Cooling Systems for Space — Status Report**

---

Peter Kittel

---

July 1984

**LIBRARY COPY**

SEP 24 1984

LANGLEY RESEARCH CENTER  
LIBRARY, NASA  
HAMPTON, VIRGINIA

**NASA**  
National Aeronautics and  
Space Administration



---

# **$^3\text{He}$ Cooling Systems for Space — Status Report**

---

Peter Kittel, Ames Research Center, Moffett Field, California



National Aeronautics and  
Space Administration

**Ames Research Center**  
Moffett Field California 94035

*N84-30226 # -*

## <sup>3</sup>He COOLING SYSTEMS FOR SPACE - STATUS REPORT

Peter Kittel

Space Technology Branch, NASA Ames Research Center, Moffett Field, CA 94035 USA

The development of a space-compatible <sup>3</sup>He refrigerator would provide a significant improvement in several areas of research /1/. One such area is infrared astronomy where the sensitivity of bolometers improves dramatically with decreasing temperature. In particular, the noise equivalent power (NEP) varies as  $T^n$ , where  $3/2 < n < 5/2$ . Compared to operating at 1.5 K, a detector operating at 0.3 K could detect a 50 times weaker signal. A second research area that would benefit is the study of critical phenomena in quantum fluids. Of particular interest is the tricritical point of <sup>3</sup>He/<sup>4</sup>He mixtures. On Earth, experiments in the region of the tricritical point are limited by gravity gradients to a resolution of  $\sim 10^{-3}$  K. Reducing gravity by four orders of magnitude would increase the resolution of experiments to  $\sim 10^{-5}$  K.

There are several methods of achieving these temperatures on Earth: <sup>3</sup>He refrigeration, dilution refrigeration, and adiabatic demagnetization refrigeration. This paper will deal with the progress of adapting <sup>3</sup>He refrigeration for use in space. While <sup>3</sup>He refrigeration has been used for a number of years in laboratories /2/, on balloons /3/, in aircraft /4/, and in spin-stabilized sounding rockets /5/, it has yet to be used in the low-gravity environment of space. Descriptions of various cycles and possible embodiments of <sup>3</sup>He refrigerators follow. Also included is an analysis of the liquid confinement and liquid-vapor phase-separation system. A possible configuration is then analyzed. Finally, the results of ground-based experiments will be discussed.

Several different refrigeration cycles are possible, including an open cycle, an intermittent-closed cycle, and a continuous-closed cycle. The embodiments of these cycles are shown in figure 1. The open cycle is the simplest, but uses the most <sup>3</sup>He. First, <sup>3</sup>He gas is condensed into the pot and then vented into space, resulting in evaporative cooling. Since the gas escapes from the system, it cannot be recycled. Thus, when the initial charge of gas is exhausted, a fresh supply must be used to restart the refrigerator. Of course, if the pot is big enough, one large charge could last the entire mission. The second system is the intermittent, closed cycle. This is a sealed system that needs to be filled only once. The adsorption pump is alternately heated and cooled to condense and evaporate the <sup>3</sup>He. The last variation is the continuous, closed cycle. The configuration in this case is similar to the configuration used in Jet Propulsion Laboratory's adsorption Joule-Thomson refrigerator /6/ and in Mikheev et al.'s dilution refrigerator /7/. Two (or more) adsorption pumps are alternately heated and cooled to provide a continuous circulation of <sup>3</sup>He through the system.

The design of most of the components of these three alternatives are well known. The principal exceptions are some of the adsorption isotherms for the pumps and the liquid containment system in the pot. The latter item is common to all of the previous designs and will be discussed in some detail next with emphasis on the intermittent, closed cycle. This cycle has been selected because of its efficiency and because most of the development work has concentrated on this type of system.

The refrigeration process is the same in the three alternatives. In all cases, warm  $^3\text{He}$  gas must be cooled until it condenses. The condensed liquid is then cooled by evaporation to reach the operating temperature. During this portion of the cycle some of the  $^3\text{He}$  is evaporated. For the cycles shown in figure 1a and 1b the mass fraction lost /8/ is

$$\Delta m/m = 1 - \exp\left(-\int_{T_0}^{T_c} C/L \, dT\right) \quad (1)$$

where  $T_c$  and  $T_0$  are the condensation and operating temperatures, respectively,  $C$  is the heat capacity, and  $L$  is the latent heat. For the cycle shown in figure 1c the loss is

$$\Delta m/m = [H(T_c) - H(T_0)]/L(T_0) \quad (2)$$

where  $H$  is the enthalpy of the liquid. These losses are shown in figure 2. The latter loss is greater because the cool-down process is inherently irreversible.

The containment of  $^3\text{He}$  has been discussed previously /9/ and will be summarized here. If the pot is filled with a porous material, then the liquid  $^3\text{He}$  could be contained by capillary attraction. This use of capillary confinement in a  $^3\text{He}$  refrigerator was first suggested by Ostermeier et al. /10/ and first demonstrated by Ennis et al. /11/. The main concerns with this type of confinement are whether the vapor can be condensed into the porous matrix without leaving large voids, and whether the liquid can be evaporated from the matrix without bubbles forming that would expel the liquid. In discussing these effects, the porous matrix will be modeled as smooth cylindrical capillaries of radius  $r$  and height  $h$  parallel to any acceleration. While real accelerations can be expected to occur in any direction, the parallel orientation is the worst case. Deficiencies in this model will be discussed.

The porous matrix serves two functions during the refrigeration cycle. It provides a large surface for the vapor condensation and for the liquid retention. Both the vapor pressure gradient and the surface tension gradient provide forces that drive the condensed liquid to the coldest place in the system. Thus, at the end of the condensation phase of the cycle, all of the liquid will be at the coldest point unless there is some other force, such as gravity, to drive the fluid elsewhere. If the cold spot is a porous matrix, then the condensation is enhanced because the surface tension is increased by the small geometry of the pores and because the increased surface area increases the condensation rate. However, there may be a difficulty when using a porous matrix. The

condensation may take place only on the outside of the matrix, leaving voids in the interior. Experiments by Donnelly et al. /12/ and Ennis et al. /11/ have not succeeded in demonstrating this effect. They showed that the condensed liquid substantially fills the matrix.

In a spacecraft the porous matrix must hold the liquid against any lateral accelerations. These accelerations, in general, can occur in any direction and be of variable magnitude. The balance between acceleration forces and surface tension forces is usually described in terms of the Bond number,  $B_0$ . The ratio of the acceleration forces to the surface tension forces,  $B_0$ , is

$$B_0 = \frac{F_a}{F_s} = \frac{\rho_l a r h}{2\sigma} \quad (3)$$

where  $a$  is the acceleration,  $\rho_l$  is the liquid density, and  $\sigma$  is the surface tension. If  $B_0 > 1$ , the acceleration forces dominate and if  $B_0 < 1$ , the surface tension forces dominate. Thus, to retain the fluid the matrix must be selected such that  $B_0 \ll 1$  for all expected accelerations. The system properties,  $B_1 = \rho_l a / 2\sigma$ , and the design parameters,  $\alpha = r h$ , can be explicitly separated, leading to the stability condition

$$\alpha \ll 1/B_1 \quad (4)$$

The function  $1/B_1$  is shown in figure 3. For any given temperature, it can readily be seen that the smaller  $r$  is, the greater  $h$  can be and thus more liquid can be held.

During the evaporation phase, bubbles that form will tend to expand, displacing and eventually expelling liquid. Since the expelled liquid will not produce any useful cooling in the system, it would be desirable to prevent the expulsion. This problem can be broken down into several parts, starting with the initial formation of the bubbles. In a porous matrix, bubbles will form by inhomogeneous nucleation at nucleation sites on the walls. Bubbles will form when the liquid temperature,  $T$ , exceeds the superheat ( $\Delta T_s = T - T_{sat}$ ). Bald /13/ has estimated the superheat, which is shown in figure 4. Bubble formation can be prevented if the temperature gradients in the fluid are kept small and the superheat is never reached. This requires the effective thermal conductance,  $K_e$ , across the fluid to be large. The effective conductance is the combined effect of the matrix and fluid acting in parallel between the heat source (where nucleation is most likely to occur) and the fluid's free surface (where evaporative cooling occurs). The temperature drop across the system is  $\Delta T = \dot{Q}/K_e$ , which must be less than the superheat. Thus the condition to be stable against the formation of bubbles is

$$\dot{Q}/K_e < \Delta T_s \quad (5)$$

Since the liquid conductivity,  $\kappa_l$ , is set by the properties of  $^3\text{He}$ , only the matrix conductivity,  $\kappa_m$ , is a free parameter. A high-conductance matrix, such as copper, will give the best stability.

If we consider the heat flux into a single capillary, then equation (5) can be expressed in terms of an equivalent conductivity  $\kappa_e$ , where  $K_e = \pi\kappa_e r^2/h$

$$\frac{h}{r^2} \ll \frac{\kappa_e \pi \Delta T_s}{\dot{Q}} \quad (6)$$

(The equivalent conductivity can also be written in terms of the liquid and matrix conductivities,  $\kappa_l$  and  $\kappa_m$ , respectively, and  $\eta$  the void fraction of the matrix:  $\kappa_e = \kappa_l + \kappa_m(1 - \eta)/\eta$ . For convenience we have modeled the combined conductors as a cylinder with the same dimensions as the fluid column.)

If a bubble does form, it will be free to move within the liquid by surface tension gradients. The surface tension gradients are the result of temperature gradients and the temperature dependence of the surface tension. The surface tension of  $^3\text{He}$  as a function of temperature is shown in figure 5. The surface tension gradient force (the Marangoni effect) will move the bubble toward the higher temperature; i.e., toward the heat source and away from the free surface of the liquid which is being evaporatively cooled. (This force is given by  $-\pi r^2 (d\sigma/dT) (dT/dx)$ .) Since the bubble most likely formed near the heat source, it will not move far if at all. Furthermore, at low temperatures  $d\sigma/dT$  approaches zero and so will the surface tension gradient force. Thus at the operating temperature there will be no force to move a bubble.

We have seen that once formed, a bubble is not likely to move; it can only grow. Fortunately, the growth of the bubbles can be controlled. To illustrate this, we will consider a bubble blocking an otherwise full capillary (figure 6). There are two forces acting on the liquid. One,  $F_p$ , is the force due to the pressure difference,  $\Delta P$ , across the liquid. If a quasi-static process is assumed where the vapor in the bubble and the vapor outside the capillary are in thermal equilibrium with their respective liquid interfaces, the Clausius-Clapeyron relation and the expression for the equivalent thermal conductance can be used to evaluate  $F_p$  as

$$F_p = \frac{\dot{Q} h \rho_v L}{\kappa_e T} \quad (7)$$

where  $\rho_v$  is the vapor density. The other force acting on the liquid is the surface tension force:  $F_s = 2\pi r \sigma$ .

To aid in determining which of the two forces dominate, we will define a dimensionless number,  $E_J$ , as the ratio of  $F_p$  to  $F_s$ :

$$E_J = \frac{\dot{Q} h \rho_v L}{2\pi r \kappa_e \sigma T} = E_1 \beta \quad (8)$$

where  $E_1 = \rho_v L / 2\pi\sigma_e T$  contains the system properties and  $\beta = \dot{Q}h/r$  contains the design parameters. If  $E_J < 1$  (or  $\beta < 1/E_1$ ) the surface tension force will dominate and the system will be stable against expulsion. A plot of  $1/E_1$  as a function of temperature is shown in figure 7 for  $^3\text{He}$  in a 50% copper matrix.

The above limitations have been applied to a hypothetical refrigerator by Kittel and Rodriguez /9/. The refrigerator was a spherical cavity of volume  $V = 4\pi h^3/3$  filled with 50% void copper matrix. The refrigerator requirements are listed in table 1. They found that these requirements lead to a series of constraints on the design parameters. These constraints are depicted in figure 8 and are discussed later. In order to provide the required cooling and sustain the pump-down losses, the volume of the liquid chamber must be  $V > 7.8 \text{ cm}^3$  for the example. Bond number considerations lead to the condition  $rh \ll 2 \text{ mm}^2$ . To avoid bubble nucleation,  $h$  must be  $> 0.7 \text{ mm}$ . Since this is so much less than the other constraint on  $h$ , it may be ignored. The last restriction comes from ejection considerations. This limits  $r/h$  to  $< 0.02$ .

Early attempts to demonstrate the refrigeration cycle at the University of Oregon /12/ showed for a variety of cryogenes that (1) gases could be condensed into a porous matrix, (2) if the pores were small enough the matrix could be substantially filled, (3) droplets were not ejected during evaporation, and (4) useful refrigeration could be achieved. Unfortunately, the researchers were not able to test all of these properties simultaneously in the appropriate environment with helium. At Ames Research Center /11/, an apparatus was built to demonstrate all of these attributes in an inverted geometry. The apparatus is shown in figure 9. To condense the helium, exchange gas is admitted to the inner vacuum space, establishing thermal contact with the helium bath. When condensation is complete the exchange gas is pumped out, breaking the thermal contact. Next, the matrix is pumped on, resulting in evaporative cooling. Several different copper matrices have been used. These have had nominal densities of 40%, 50%, and 60%, and typical pore sizes of  $10 \mu\text{m}$ . This apparatus has been used for both  $^3\text{He}$  and  $^4\text{He}$ , resulting in minimum temperatures of 0.5 K and 1.4 K, respectively. The complete refrigeration cycle has been demonstrated. It was shown that the matrix could be completely filled by condensation and that useful refrigeration could be achieved without the expulsion of liquid. At high heat fluxes, deviations from ideal behavior were observed in the 60% sponge. The cause of this deviation is not known.

In conclusion, it is feasible to design a  $^3\text{He}$  refrigerator that will operate in the low-gravity environment of space where accelerations can occur in random directions. The key to the design is to fill the liquid chamber with a high-conductivity porous material such as sintered copper. The pores allow the surface tension forces to contain the liquid, while the high conductivity ensures that the vaporization occurs at the surface of the matrix rather than internally. The matrix also provides a favorable place for condensation to occur and suppresses bubble nucleation and movement.

I would like to acknowledge R. J. Donnelly and his group at the University of Oregon; D. J. Ennis and W. F. Brooks of Ames Research Center; A. F. Rodriguez of the University of the Pacific;

A. L. Spivak of Trans-Bay Electronics; numerous students from the University of California at Santa Cruz for their contributions to this work; and the NASA Office of Aeronautics and Space Technology for their support.

#### REFERENCES

1. P. Kittel, Adv. Cryo. Eng. 27, 745 (1982).
2. G. Chanin, J. P. Torre, Proc. Sixth Int. Cryo. Eng. Conf., (IPC Science and Technology Press, Guildford, 1976) 96.
3. D. P. Woody, P. L. Richards, Phys. Rev. Lett. 42, 925 (1979).
4. J. V. Radostitz, I. G. Nolt, P. Kittel, R. J. Donnelly, Rev. Sci. Instrum. 49, 86 (1978).
5. H. Gush, Proc. Space Helium Dewar Conference (to be published, U. of Alabama Press, 1984).
6. J. A. Jones, Refrigeration for Cryogenic Sensors, NASA CP-2287, 357 (1983).
7. V. A. Mikheev, V. A. Maidanov, N. P. Mikhin, Cryogenics 24, 190 (1984).
8. P. Kittel, W. F. Brooks, Adv. Cryo. Eng. 27, 727 (1982).
9. P. Kittel, A. F. Rodriguez, NASA TM-85973 (1984).
10. R. M. Ostermeier, I. G. Nolt, J. V. Radostitz, Cryogenics 18, 83 (1978).
11. D. J. Ennis, P. Kittel, W. A. Brooks, A. Miller, A. L. Spivak, Refrigeration for Cryogenic Sensors, NASA CP-2287, 405 (1983).
12. R. J. Donnelly, P. Kittel, R. M. Ostermeier, J. V. Radostitz, B. R. Lee, J. C. Cooper, Final Report, NASA Grant NSG-2208 (1979).
13. W. B. Bald, Pre-existing Gaseous Phase, Dept. of Engineering Report N-75-29279, (U. of Oxford, 1975).

Table 1  
Refrigerator Requirements

Parameter	Symbol	Value
Condensation temperature	$T_c$	2 K
Operating temperature	$T^o$	0.3 K
Hold time	$t^o$	54 ks
Refrigeration power*	$Q_p$	40 $\mu$ W
Peak acceleration	$a$	0.1 g

\*Includes parasitic loads



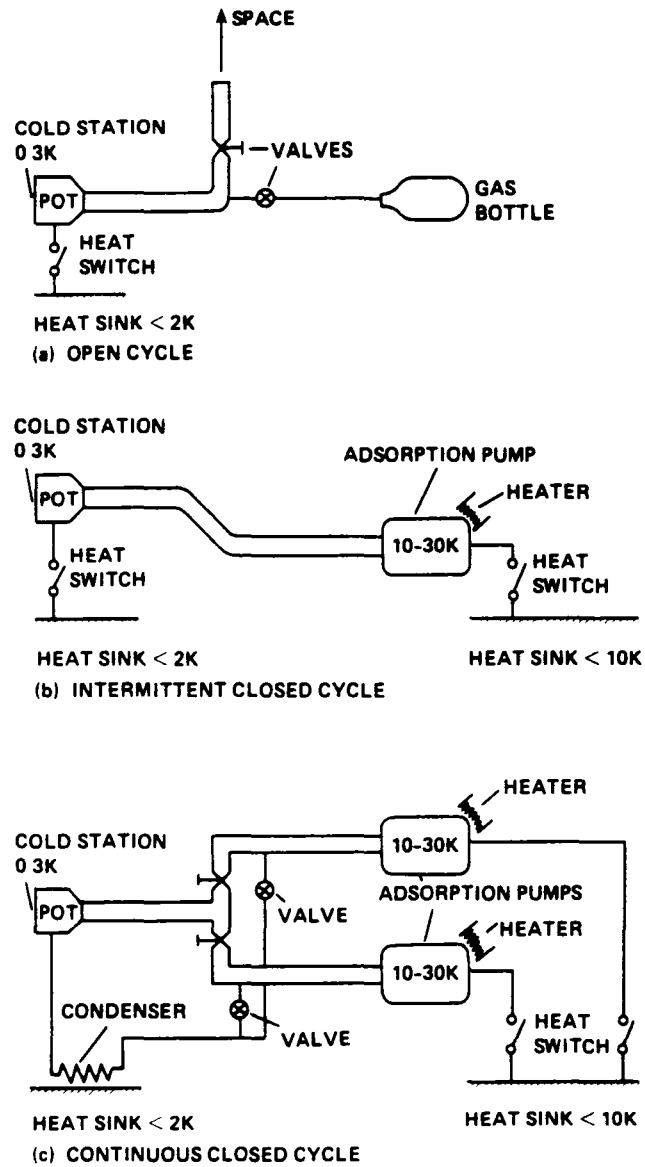


Fig. 1 Principal components of three possible embodiments of a  $^3\text{He}$  refrigerator.

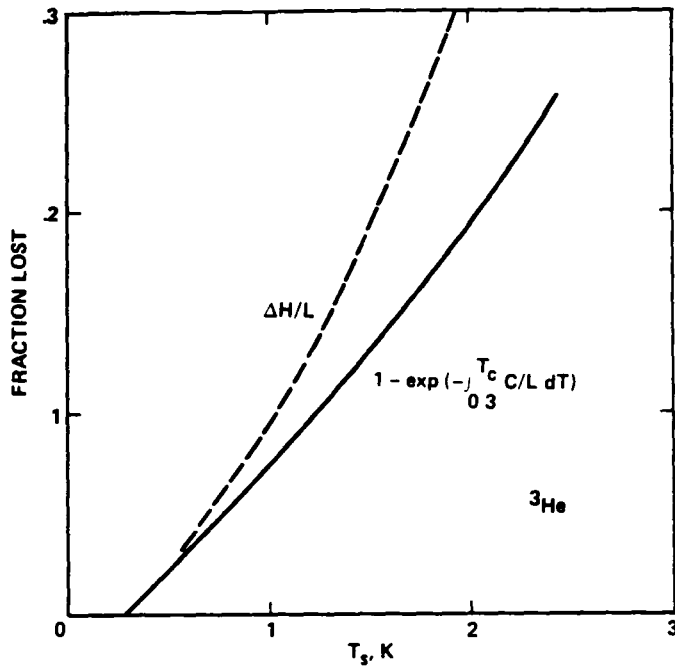


Fig. 2 Fraction of  $^3\text{He}$  moved in evaporative cooling from  $T_c$  to 0.3 K. The solid line is for noncontinuous cycles and the dashed line is for continuous cycles.

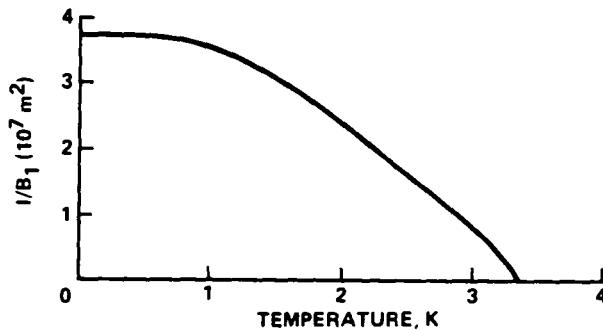


Fig. 3 Plot of  $1/B_1$  as a function of temperature for the case where the acceleration is  $9.8 \text{ m/s}^2$ . The regions below the curves are regions at which surface tension forces dominate.

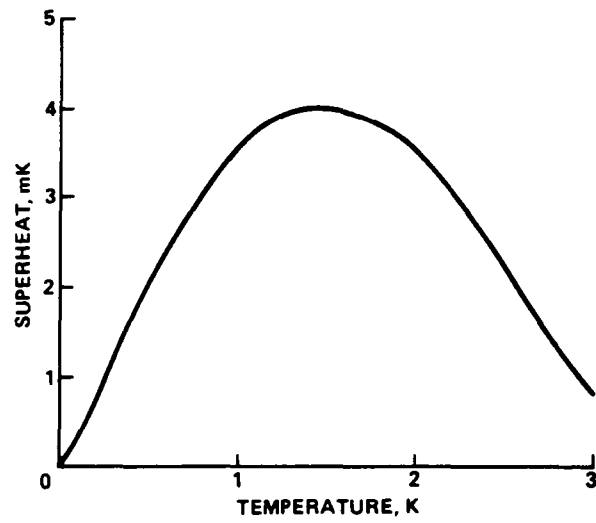


Fig. 4 Superheat as a function of temperature.

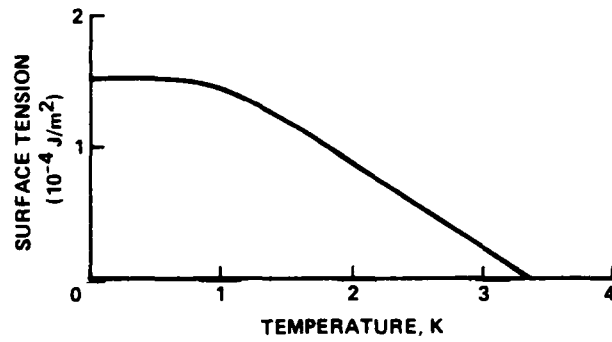


Fig. 5 Surface tension as a function of temperature.

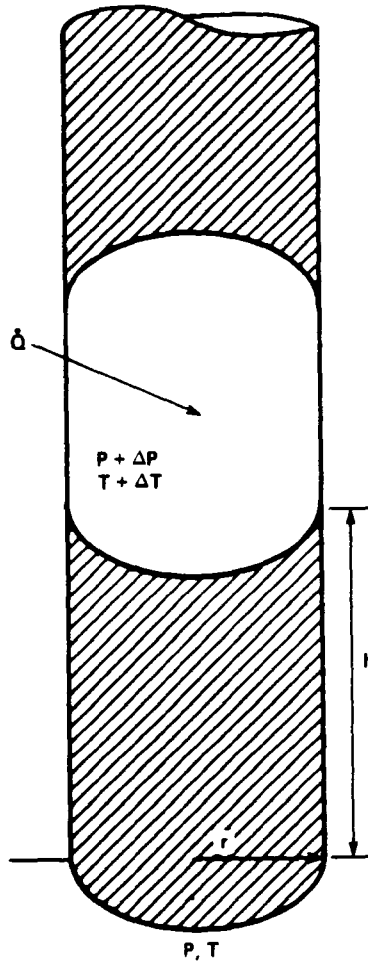


Fig. 6 A vapor bubble blocking an otherwise full capillary. The capillary has a radius,  $r$ . A column of liquid of height,  $h$ , separates the bubble from free space. A temperature difference of  $T$  and a pressure difference of  $P$  are across the liquid column. There is a heat flux of  $Q$  into the bubble.

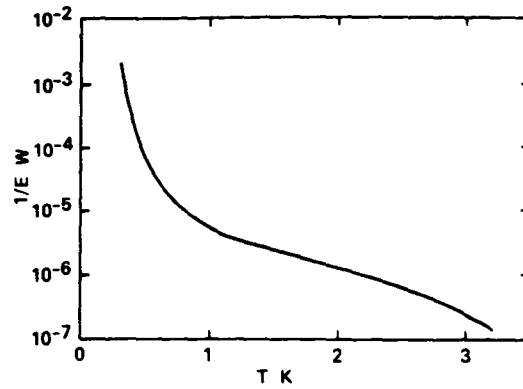


Fig. 7 Plot of  $1/E_1$  as a function of temperature where a 50% density copper matrix has been assumed.

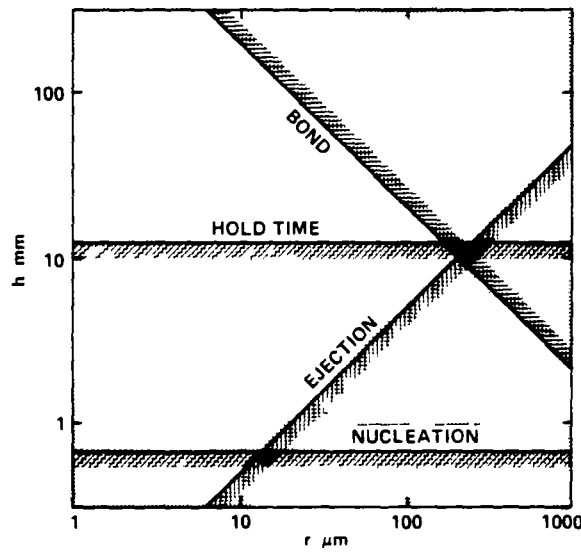


Fig. 8 Stable and unstable regions of  $r$ - $h$  space for various types of instabilities. Shading indicates the region of instability.

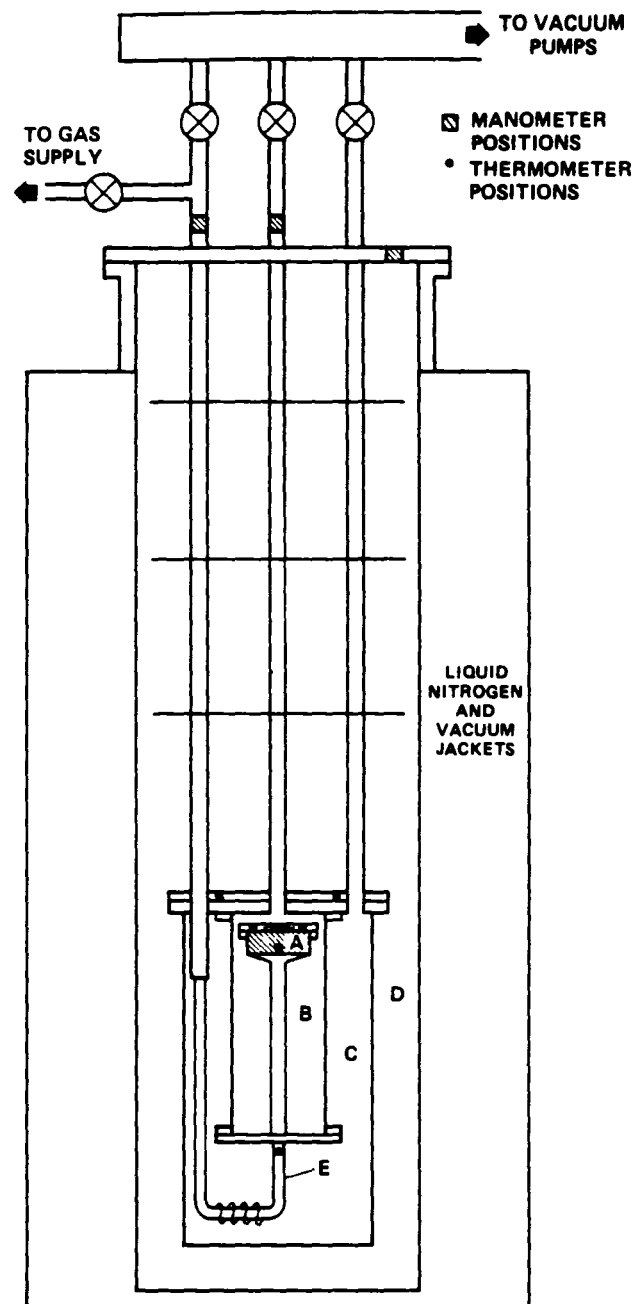


Fig. 9 Diagram of capillary confinement cryostat.

1 Report No NASA TM-85985	2 Government Accession No	3 Recipient's Catalog No	
4 Title and Subtitle <sup>3</sup> HE COOLING SYSTEMS FOR SPACE--STATUS REPORT		5 Report Date July 1984	
		6 Performing Organization Code	
7 Author(s) Peter Kittel		8 Performing Organization Report No A-9821	
		10 Work Unit No T-6624	
9 Performing Organization Name and Address Ames Research Center Moffett Field, CA 94035		11 Contract or Grant No	
		13 Type of Report and Period Covered Technical Memorandum	
12 Sponsoring Agency Name and Address National Aeronautics and Space Administration Washington, DC 20546		14 Sponsoring Agency Code 506-54-21	
		15 Supplementary Notes Point of Contact: Peter Kittel, Ames Research Center, MS 244-7, Moffett Field, CA 94035 (415) 965-6525 or FTS 448-6525	
16 Abstract The development of a space-compatible <sup>3</sup> He refrigerator would provide a significant improvement in several areas of research in the 0.3 to 1 K temperature range. There are several methods of achieving these temperatures on Earth: <sup>3</sup> He refrigeration, dilution refrigeration, and adiabatic demagnetization refrigeration. This paper will deal with the progress of adapting <sup>3</sup> He refrigeration for use in space. Various cycles and possible embodiments of <sup>3</sup> He refrigerators are described. Also included is an analysis of the liquid confinement and liquid-vapor phase-separation system. A possible configuration is then analyzed. Finally, the results of ground-based experiments will be discussed.			
17 Key Words (Suggested by Author(s)) Refrigeration Helium 3 Capillary Porous media		18 Distribution Statement Unlimited  Subject Category - 34	
19 Security Classif (of this report) Unclassified	20 Security Classif (of this page) Unclassified	21 No of Pages 15	22 Price* A02

**End of Document**